Journal of Immunological Methods 465 (2019) 39–44

Contents lists available at ScienceDirect

Journal of Immunological Methods

journal homepage: www.elsevier.com/locate/jim

High-sensitivity lateral flow immunoassay with a fluorescent lanthanide nanoparticle label

Teppo Salminen*, Etvi Juntunen, Sheikh M. Talha, Kim Pettersson

Department of Biotechnology, University of Turku, Turku, Finland

ARTICLE INFO

Keywords:
Prostate specific antigen
Lateral flow
Fluorescent
Immunoassay

ABSTRACT

Lateral flow (LF) immunoassays are commonly used for point-of-care testing and typically incorporate visually read reporters, such as gold particles. To improve sensitivity and develop quantitative LF immunoassays, visual reporters can be replaced by fluorescent reporters detected by an instrument. In this study, we used fluorescent europium(III) chelate doped nanoparticle (Eu-np) reporters to develop a quantitative high-sensitivity LF immunoassay for free prostate specific antigen (fPSA). Furthermore, we tested different simplified formats of the assay and the effect of different modifiable parameters on the detection limit of the assay: dynamic range, assay duration and number of assay steps. The molar detection limits of the different assay formats were compared with published detection limits of LF immunoassays with different reporters. The cutoff was calculated from 11 female serum samples. The detection limit of the sensitivity optimized fPSA assay with fPSA spiked into pooled female serum was 0.01 ng/ml, which is approximately 100-fold lower than the most sensitive gold particle LF assays and 10-fold lower than other Eu-np and carbon nanoparticle based LF immunoassays. Thus, Eu-np reporters can be used to develop highly sensitive and quantitative LF immunoassays.

1. Introduction

Lateral flow (LF) immunoassays have long been considered ideal for point-of-care testing of diseases and environmental samples due to their simplicity and ease of use. Typically, LF immunoassays use visually read reporters, such as blue latex beads, carbon black nanoparticles, silver enhanced gold and, most importantly, colloidal gold nanoparticles (Linares et al., 2012). To improve the sensitivity of the LF assays, magnetic and fluorescent reporters have also been incorporated into LF assays as reporters. These reporters require an instrument for detection, which increases the price and complexity of the test. On the other hand, an instrument-based read-out also provides the advantages of quantification and objective interpretation of the results. Additionally, the instrument can archive and transmit the results automatically. These advantages decrease the risk of operator mistakes and thus many LF assays with traditional visually read reporters have also incorporated automated readers.

However, despite these recent reporter improvements the current LF immunoassays still lack the sufficiently precise quantitation and high sensitivity needed to meet the performance of central laboratory assays. Additionally, these goals of quantitation and sensitivity should be met with a sufficiently simple assay protocol in order to retain the simplicity advantage of LF immunoassays. Previously, we have shown that the LF immunoassay sensitivity and signal-to-noise ratio can be improved significantly with fluorescent europium(III) chelate doped nanoparticles (Eu-np) as reporters (Juntunen et al., 2012). Some demonstrations of LF immunoassays for different biomarkers using Eu-np reporters have also been published (Rundstrom et al., 2007; Nabatiyan et al., 2010; Xia et al., 2009; Salminen et al., 2018; Song et al., 2013). Also, Eu-np can provide a 100-fold improvement in sensitivity when comparing Eu-np and colloidal gold nanoparticles in the same LF test with identical binders (Xia et al., 2009; Zhang et al., 2014). In addition to Eu-np, quantum dot fluorescent nanoparticles have provided sensitivity improvements in LF when compared to colloidal gold (Di Nardo et al., 2016; Foubert et al., 2017). Even colloidal gold nanoparticle label sensitivity can be improved, by improving the visual intensity of the signal with gold-nanoparticle-decorated silica nanorods or dual gold label assays (Xu et al., 2014) (Choi et al., 2010).

In this study, we explore the critical parameters of a LF immunoassay, which affect the dynamic range, assay duration, number of assay steps and sensitivity of the final test. Significant improvements in these aspects of the assay are possible by substituting the normal visual reporters with fluorescent reporters. The LF assay format also has inherent limitations that can be charted through systematic testing of different parameters of the assay. In order to demonstrate the potential of Eu-np reporters and chart the limitations of simple yet sensitive LF

* Corresponding author at: Department of Biotechnology, University of Turku, Kiinamyllynkatu 10, FI-20520 Turku, Finland.
E-mail address: tjsalm@utu.fi (T. Salminen).

https://doi.org/10.1016/j.jim.2018.12.001
Received 5 October 2018; Received in revised form 3 December 2018; Accepted 3 December 2018
Available online 04 December 2018

assays with a real immunoassay, we developed a highly sensitive yet simple and rapid LF assay for free prostate specific antigen (fPSA).

Prostate-specific antigen (PSA) is a human kallikrein protease produced in prostatic epithelial cells (Yousef and Diamandis, 2002). The level of PSA in blood is an important marker for early detection of prostate cancer and also for the recurrence of the cancer after treatment (Heidenreich et al., 2008). Current central laboratory PSA immunoassays have limits of detection between 0.008 ng/ml and 0.07 ng/ml (Sharma et al., 2017). PSA in the bloodstream occurs in complexed (65–95% of total PSA) and free (5–35%) forms (Lilja et al., 1991). The ratio of fPSA to total PSA in blood can be used to aid the distinguishing of prostate cancer from benign prostatic hyperplasia (Peltola et al., 2011). For example, if the total PSA level is between 4 and 10 ng/ml, a cut-off of < 25% fPSA can be used to select patients for biopsy (Catalona et al., 1994). Therefore, a specific fPSA measurement is a useful addition to diagnosis of prostate cancer, along with other PSA based serum markers (Stephan et al., 2014). However, in this study the fPSA assay functions also as a model analyte for exploring the improvements to LF immunoassays gained by using fluorescent reporters.

2. Materials and methods

2.1. Preparation of assay materials

Polyclonal mouse IgG (Biodesign, Saco, ME, USA) and H117 mouse monoclonal anti-PSA antibody (University of Turku) were covalently coupled with biotin isothiocyanate (BITC) to form biotinylated conjugates. The conjugation reaction contained 2 mg/ml of the antibody and a 100-fold excess of BITC in 50 mM carbonate buffer (pH 9.8). The reaction was incubated for 4 h at room temperature and excess BITC was separated from the conjugate by NAP-5 and NAP-10 columns (Amersham Pharmacia Biotech, Uppsala, Sweden), with the biotin-antibody conjugates eluted to 10 mM Tris-HCl buffer (pH 8.0).

Carboxyl-modified Eu(III)-chelate-doped OptiLink polystyrene nanoparticles with a diameter of 107 nm (Seradyn, Indianapolis, IN, USA) were covalently linked with anti-PSA antibody 5A10, which binds to an epitope specific for free PSA (Pettersson et al., 1995), and with both biotinylated and non-biotinylated polyclonal mouse-IgG (Biodesign, Saco, ME, USA), as described previously (Soukka et al., 2001a). The resulting anti-PSA-Eu nanoparticles and bio-mIgG-Eu nanoparticles were used as reporters in the LF assays. The recombinant PSA used as standard was produced and purified as described by Rajakoski et al. (Rajakoski et al., 1997).

The test and control lines on the LF strips were printed with a Linomat 5 non-contact printer (CAMAG, Muttenz, Switzerland) onto a Hi-Flow Plus HF180 or HF90 nitrocellulose membrane (Millipore, Bedford, MA, USA). The streptavidin (SA) test lines were printed in 10 mM citrate-phosphate buffer (pH 5.0). The biotinylated PSA capture antibody H117 was printed in 10 mM Tris-HCl buffer (pH 8.0), with an optimized final density of 0.25 µg/cm (result not shown). The control line of 0.4 µg/cm of rabbit—anti-mouse polyclonal antibody was printed at a distance of 6 mm from the test line in 10 mM Tris-HCl buffer (pH 8.0). Before printing the lines, the nitrocellulose membrane was attached to an adhesive backing plastic (G&L Precision Die Cutting, San Jose, CA, USA). After printing, the membranes were dried in + 35 °C for 2 h. Subsequently, a cellulose absorption pad (Millipore) and a glass fiber feed pad were attached overlapping the nitrocellulose. This assembled membrane card was then cut into 5 mm wide lateral flow strips.

The reaction buffer used for reagent dilutions and wash steps consisted of 10 mM phosphate buffer (pH 7.4), 135 mM NaCl, 0.5% Polysorbate 20, 1% BSA (Bioreba, Reinach, Germany). The female serum samples used for measurement of blank signal were from informed healthy volunteer donors.

2.2. Streptavidin test line optimization

Different densities of SA ranging from 0.5 to 128 µg/cm were printed and dried on the LF strips. The density of SA was calculated in micrograms per centimeter of test line, each strip containing a 5 mm test line. Optimal SA density was tested by performing an assay with bio-mIgG and mIgG coated Eu-nanoparticles on the SA LF strips not containing the biotinylated capture antibody. Firstly, 10^7 bio-mIgG or mIgG coated Eu-nanoparticle reporters per strip were added to the SA LF strips in 20 µl of reaction buffer, together with 18 nmol of d-biotin per strip. Adding this high concentration of d-biotin to block a constant portion of the binding sites was necessary to ensure that the bio-mIgG nanoparticles were not the limiting reagent in the assay. This is because the SA line contains a much higher number of biotin binding sites than the total number of biotin molecules on the bio-mIgG nanoparticles. Using only bio-mIgG nanoparticles would have resulted in a constant signal from lines with different concentrations of SA, since the usable concentrations of bio-mIgG nanoparticles are too low to saturate the SA line.

Secondly, after reporter absorption the strips were washed by adding 80 µl of reaction buffer. After reaction buffer absorption, the strips were dried in room temperature and the long-lifetime Eu(III)-chelate fluorescence was measured with a Victor X4 multilabel reader (Perkin-Elmer/Wallac, Turku, Finland) in a time-resolved europium measurement.

2.3. LF fPSA assay procedure

In the standard LF fPSA assay procedure, 10 µl of PSA spiked pooled female serum sample and 20 µl of reaction buffer containing 10^8 particles of anti-PSA-Eu were added to each strip. Immediately after adding the anti-PSA-Eu, the strip was washed by adding 20 µl of reaction buffer and left to run in room temperature for 25 min before measurement. In the signal development assay, the strips were measured sequentially approximately every 70 s after adding the sample and reporter. The measurement was repeated during the liquid flow through the membrane for a total of 27 min. All assays had spiked pooled female serum as the sample matrix.

3. Results

3.1. Density of streptavidin test line

The optimal streptavidin density on the test line was tested by comparing the capacity of different density lines to bind bio-mIgG-Eu nanoparticles with the unspecific binding of mIgG-Eu nanoparticles. The bio-mIgG-Eu nanoparticles show the actual relevant binding capacity for nanoparticle reporters; the actual biotin binding capacities of the various densities of SA line may be higher, but steric hindrances caused by the large sized nanoparticles should lower the effective binding capacity. The nanoparticle binding capacity of the SA line increases up to a density of 8–16 µg/cm of SA (Fig. 1). Taking the mIgG-Eu nanoparticle background into account, the maximal signal-to-background ratio is achieved between 4 and 16 µg/cm of SA. LF strips with 4 µg/cm of SA were used in the fPSA assays.

3.2. Detection limits of different types of assays

The limit of detection (LoD) was calculated from the standard curve, with the cutoff calculated by the following equation:

$$LoD = \mu_B + 1.645\sigma_B + 1.645\sigma_S$$

where μ_B is the mean of blank measurements, σ_B is standard deviation of blank measurements and σ_S is the standard deviation of low sample concentration measurements. The blank signal was the average signal of 11 measured female sera with a total of 99 replicates. The LoD was

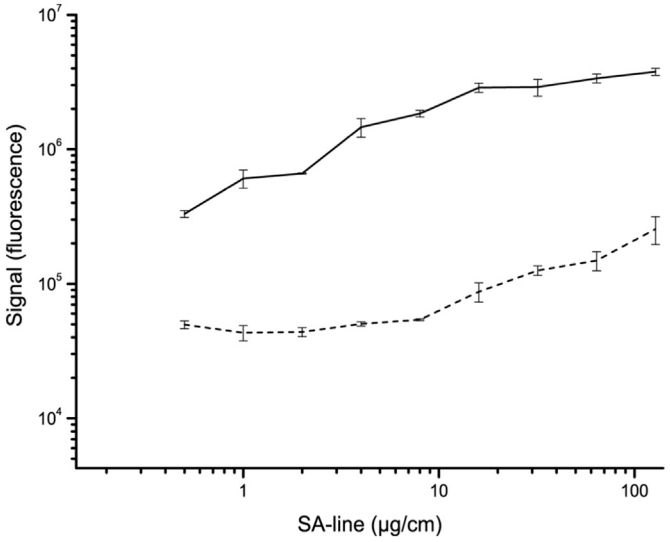

Fig. 1. The binding capacity and background of streptavidin test lines with different concentrations of streptavidin. Solid line shows the nanoparticle binding capacity of streptavidin lines with different concentrations of streptavidin, tested by adding biotinylated mouse-IgG coated Eu(III)-nanoparticles on the strip. Dashed line shows the unspecific nanoparticle binding on streptavidin lines, tested with non-biotinylated but otherwise identical mouse-IgG coated Eu (III)-nanoparticles. Standard deviations of three replicates are depicted as error bars. The streptavidin concentration chosen to be used in subsequent assays was 4 µg/cm.

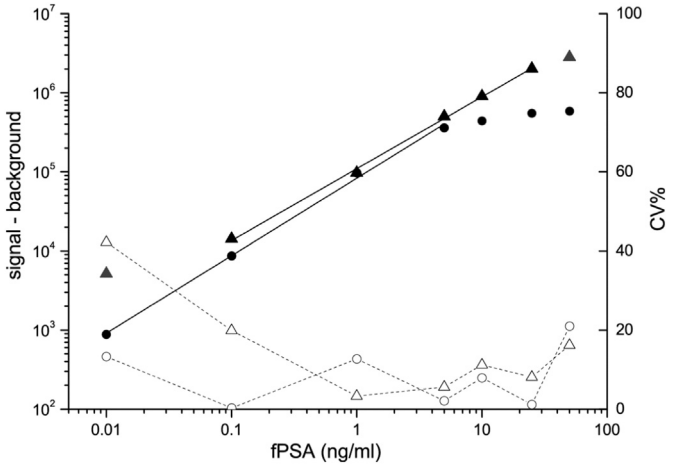

Fig. 2. fPSA LF assay dynamic range with 10^8 particles/strip (●) and 10^9 particles/strip (▲) of the anti-PSA-Eu nanoparticle reporter. With 10^8 and 10^9 nanoparticles per strip, the assay is linear up to 5 ng/ml and 25 ng/ml of fPSA, respectively. Coefficients of variation (%) with three replicates are shown with dashed lines and empty symbols.

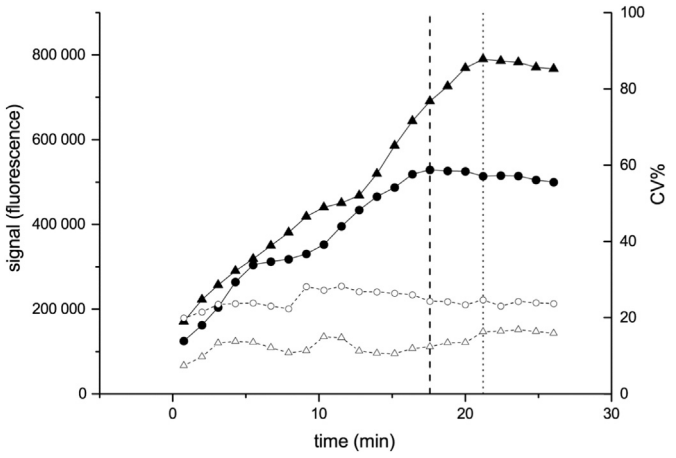

Fig. 3. Signal development after adding the sample to the strip in the fPSA assay with HF75 (●) and HF180 (▲) nitrocellulose membranes used in the assays. The assay reached maximum signal after 17 min (dashed line) with HF75 nitrocellulose and after 21 min (dotted line) with HF180 nitrocellulose. Coefficients of variation (%) with three replicates are shown with dashed lines and empty symbols.

tested for the sensitivity optimized fPSA LF assay and three variations of the assay protocol (Table 1). The assay optimized for high sensitivity had a LoD of 0.01 ng/ml.

To test the possibility of shifting the dynamic range of the assay to higher concentrations, reporter Eu-np amount was increased ten-fold to 10^9 particles/strip. Compared to the assay with 10^8 particles/strip, the upper limit of linearity increased from 5 to 25 ng/ml of PSA (R-square 0.998 for both Eu-np amounts) (Fig. 2). The LoD with the higher nanoparticle amount was 0.063 ng/ml.

In order to decrease the time the assay takes to reach the maximum signal level, the flow speed of the sample and reporter conjugate was increased by using a larger pore size nitrocellulose membrane. The assay with the faster flow speed HF75 nitrocellulose reached maximum signal after 17 min, compared to the 21 min of the normal assay with HF180 nitrocellulose (Fig. 3). The LoD with HF75 nitrocellulose was 0.014 ng/ml.

The standard assay protocol included a wash step comprising 20 µl/strip of reaction buffer. When the assay was simplified by eliminating this wash step, the LoD was 0.058 ng/ml (Fig. 4).

4. Discussion

In this study, we have developed a highly sensitive LF assay for fPSA with fluorescent Eu-nanoparticles as reporters. The most sensitive variation of the assay protocol had a limit of detection of 0.010 ng/ml (3.5×10^{-13} M). We also tested the assay with different simpler assay protocol variations to test the effect of these parameters on the sensitivity of the assay. The LoD in these protocols varied from 0.014 to 0.058 ng/ml 5.1×10^{-13} - 20×10^{-13} M) (Table 1). The simplification of the assay protocols consisted of removing the wash step to achieve a one-step protocol and using a fast nitrocellulose to decrease the time

Table 1
The limits of detection of the different variations of fPSA LF assays. Sensitivity optimized assay is the baseline for the other variations and 10^9 particles/strip is tested in order to shift the dynamic range. Using a fast HF75 nitrocellulose shortens the assay time and removing the wash simplifies the assay. The limit of detection is shown for each variation in ng/ml and mol/L. The assay modifications reduce the turnaround time and the number of steps needed to complete the assay but result in increased limits of detection.

Assay protocol:	Limit of detection (ng/ml):	Molarity at Detection limit (M)	Turnaround Time (min)	Number of assay Steps
Sensitivity optimized assay	0.010	3.5×10^{-13}	21	2
10^9 particles/strip	0.063	22×10^{-13}	21	2
Fast HF75 nitrocellulose	0.014	5.1×10^{-13}	17	2
No wash	0.058	20×10^{-13}	21	1

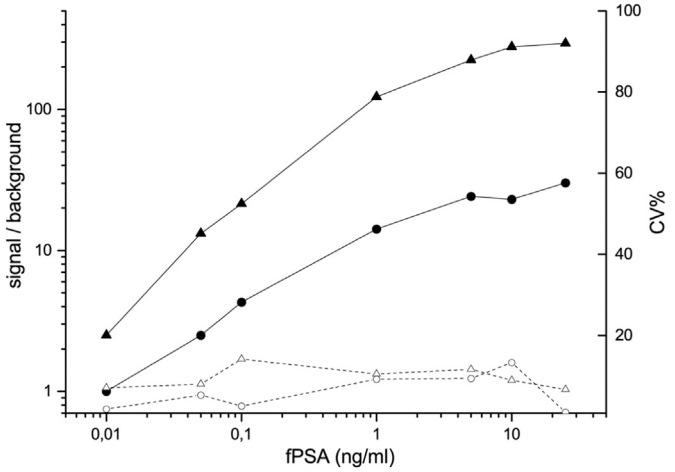

Fig. 4. fPSA LF assay signal/background ratio with a wash step (▲) and without a wash step (●). The LoD with and without a wash step is 0.01 ng/ml and 0.058 ng/ml, respectively. Coefficients of variation (%) with three replicates are shown with dashed lines and empty symbols.

the assay takes to reach the maximum signal.

Most published LF assays for PSA set the cutoff at the clinically relevant 4 ng/ml concentration of total PSA and thus do not optimize the assay for high analytical sensitivity (Miano et al., 2005; Berg et al., 2001; Dok An et al., 2001; Jung et al., 1999). However, ultrasensitive PSA assays can help in early detection of prostate cancer recurrence after radical prostatectomy, and some very sensitive PSA assays have been developed (Tilki et al., 2015). Li et al. developed a quantitative LF assay for PSA with quantum dot nanobead-labels, achieving a sensitivity of 0.33 ng/ml (1×10^{-11} M) (Li et al., 2014). Additionally, some published microtiter well-based immunoassays for PSA using different reporter technologies have reported very low limits of detection. Particularly, Soukka et al. used Eu-np reporters similar to the particles used in this publication for ultrasensitive detection of fPSA in wells achieving a limit of detection of 1.3×10^{-15} M with 30 µl of sample (Soukka et al., 2001b). With 5 µl of sample, the limit of detection was 1.3×10^{-14} M, which is equivalent to 59 zmol of fPSA in the sample. The corresponding lowest detected amount in our fPSA LF assay with 10 µl sample volume was 3500 zmol. Also, published ELISA and chemiluminescence-reporter assays for fPSA had sensitivities in the same range as the fPSA LF assay, 2.7×10^{-13} M for the ELISA and 2.3×10^{-13} M for the chemiluminescence well assay (Matsumoto et al., 1999; Liu et al., 2016). However, the sensitivity of different assays even for the same analyte is not affected only by the assay type or the label, but also the choice of binders. Therefore, direct label comparison between assays is difficult.

Taking this limitation into account, the limit of detection of our developed LF immunoassay can also be compared to other LF immunoassays for different protein markers, with the published limits of detection converted to molarity as shown by Gordon and Michel (Gordon and Michel, 2008). In their review, the detection limits of LF immunoassays based on gold particle reporters varied from 10^{-5} to 3×10^{-11} M. However, various types of reporters used in LF immunoassays have achieved lower detection limits compared to gold reporters.

LF immunoassays using Eu-np reporters for various analytes achieved detection limits down to the 10^{-12} M range (Rundstrom et al., 2007; Xia et al., 2009; Song and Knotts, 2008; Shao et al., 2017). Carbon nanoparticle based assays had similar detection limits of approximately 10^{-12} M (van Dam et al., 2004; Koets et al., 2006; Parpia et al., 2010). Experimental LF assays for bacterial toxins using dye-containing liposomes with toxin receptors incorporated in the lipid bilayer as reporters reached detection limits of 10^{-12} and 10^{-16} M (Ahn-Yoon et al., 2004; Ahn-Yoon et al., 2003). Finally, LF immunoassays with up-converting phosphor reporters had detection limits ranging from 10^{-12} to 10^{-15} M (Hampl et al., 2001; Corstjens et al., 2011; Corstjens et al., 2008; Juntunen et al., 2015).

However, there are naturally a number of limitations to an approach where different LF immunoassay reporters are compared across a variety of protein markers and publications. First, each protein marker has different binder antibodies with different affinities. Secondly, the assay protocols, materials and time to results vary among assays. Thirdly, assays for different proteins have been tested in different sample matrices, some of which may be more challenging for the assays than others. Finally, even the methods used to determine the detection limit vary among the published assays. Nevertheless, a broad comparison between different reporter types can be made. When compared to the other published LF immunoassays, the lowest detection limit of 3.5×10^{-13} M achieved with our published fPSA LF immunoassay is approximately 100-fold lower than the most sensitive gold particle LF assays and 10-fold lower than other Eu-np and carbon nanoparticle based LF assays. A similar or even superior detection limit can be reached with up-converting phosphor reporters.

Like all fluorescent reporters, Eu-nanoparticles require an instrument for detection. In addition to the sensitivity enhancement of instrument-based reading, use of an instrument also enables quantitative assays and lowers the possibility of human error in result reading and data management (Scherr et al., 2016). Because of these advantages, even LF assays with visually readable gold particle reporters are often read by an optical instrument. Due to the conflicting needs of sensitive intrumentation and portability as wells as affordability, the practical success of fluorescence based LF immunoassays is largely dependent on the availability of low-cost miniaturized detection instruments. This need for portable LF readers capable of detecting Eu-nanoparticle labels is already being met. For example, an LF immunoassay for influenza using Eu-np reporters together with a dedicated reader is in the market (Lee et al., 2012; Leonardi et al., 2013). Also, published LF immunossays with Eu-np reporters have used commercially available portable readers (Song et al., 2013; Shao et al., 2017; Liang et al., 2017) or even a digital camera together with an ultraviolet light source (Juntunen et al., 2012; Xia et al., 2009; Xia et al., 2013) as a detection instrument. Uniquely, Preechadakasedkit et al. developed reporter particles with a gold core coated with europium chelate-doped silica coating, allowing both visual and instrument-based fluorescent detection in a LF assay (Preechakasedkit et al., 2018).

In rapid point-of-care assays, the critical parameters that affect the limit of detection force a compromise between sensitivity on one hand and speed and simplicity on the other. Particularly the elimination of a separate wash step simplifies the assay but also increases the limit of detection from 0.01 ng/ml to 0.058 ng/ml. Additionally, the adjustment of the dynamic range for samples with higher concentrations of the analyte may affect the sensitivity of the assay. In the case of our LF immunoassay, the dynamic range is approximately three orders of magnitude. This forces a compromise in the detection limit in a quantitative assay depending on the desired quantitative range. A tenfold increase in the number of reporter particles increases upper limit of linearity approximately five-fold, with a similar increase in the detection limit (Fig. 2).

The time for the sensitivity optimized assay to reach the stable maximum signal is 21 min (Fig. 3). This time can be shortened by using a nitrocellulose membrane with a larger average pore size and thus faster flow rate. The effect of using larger pore size nitrocellulose is modest; use of HF75 nitrocellulose, which has a 2.4-fold faster flow rate compared with HF180, only decreases the assay time by 4 min, from 21 min to 17 min, while increasing the detection limit from 0.010 ng/ml to 0.014 ng /ml. In order to shorten the assay time, the assay can also be measured before the maximum signal is reached. However in this case, in addition to a compromise in sensitivity, the calibration curve for a quantitative assay has to be adjusted to the exact measurement time

point due to constant change in the signal level caused by ongoing flow in the membrane.

In conclusion, it is possible to develop a highly sensitive quantitative lateral flow assay for fPSA by using fluorescent reporters. In order to achieve a simple and fast assay, a compromise has to be made between ease of use and sensitivity. Nevertheless, even in the simplest format, the developed assay is quantitative and the very sensitive compared to a LF assay based on standard gold particle reporters.

Declarations of interest

None.

This research did not receive any specific grant from funding agencies in the public, commercial, or not-for-profit sectors.

References

Ahn-Yoon, S., Decory, T.R., Baeumner, A.J., Durst, R.A., 2003. Ganglioside-liposome immunoassay for the ultrasensitive detection of cholera toxin. Anal. Chem. 75, 2256–2261.

Ahn-Yoon, S., Decory, T.R., Durst, R.A., 2004. Ganglioside-liposome immunoassay for the detection of botulinum toxin. Analytical and bioanalytical chemistry 378, 68–75. https://doi.org/10.1007/s00216-003-2365-4.

Berg, W., Linder, C., Eschholz, G., Schubert, J., 2001. Pilot study of the practical relevance of a one-step test for prostate-specific antigen in capillary blood to improve the acceptance rate in the early detection program of prostate carcinoma. Int. Urol. Nephrol. 32, 381–388.

Catalona, W.J., Hudson, M.A., Scardino, P.T., Richie, J.P., Ahmann, F.R., et al., 1994. Selection of optimal prostate specific antigen cutoffs for early detection of prostate cancer: Receiver operating characteristic curves. J. Urol. 152, 2037–2042.

Choi, D.H., Lee, S.K., Oh, Y.K., Bae, B.W., Lee, S.D., et al., 2010. A dual gold nanoparticle conjugate-based lateral flow assay (LFA) method for the analysis of troponin I. Biosens. Bioelectron. 25, 1999–2002. https://doi.org/10.1016/j.bios.2010.01.019.

Corstjens, P.L., van Lieshout, L., Zuiderwijk, M., Kornelis, D., Tanke, H.J., et al., 2008. Up-converting phosphor technology-based lateral flow assay for detection of Schistosoma circulating anodic antigen in serum. J. Clin. Microbiol. 46, 171–176 (doi:JCM.00877-07 [pii]).

Corstjens, P.L., de Dood, C.J., van der Ploeg-van Schip, J.J., Wiesmeijer, K.C., Riuttamaki, T., et al., 2011. Lateral flow assay for simultaneous detection of cellular- and humoral immune responses. Clinical biochemistry 44, 1241–1246. https://doi.org/10.1016/j.clinbiochem.2011.06.983.

Di Nardo, F., Anfossi, L., Giovannoli, C., Passini, C., Goftman, V.V., et al., 2016. A fluorescent immunochromatographic strip test using Quantum Dots for fumonisins detection. Talanta 150, 463–468. https://doi.org/10.1016/j.talanta.2015.12.072.

Dok An, C., Yoshiki, T., Lee, G., Okada, Y., 2001. Evaluation of a rapid qualitative prostate specific antigen assay, the one step PSA(TM) test. Cancer Lett. 162, 135–139 (doi:S0304383500006157 [pii]).

Foubert, A., Beloglazova, N.V., De Saeger, S., 2017. Comparative study of colloidal gold and quantum dots as labels for multiplex screening tests for multi-mycotoxin detection. Anal. Chim. Acta 955, 48–57. https://doi.org/10.1016/j.aca.2016.11.042.

Gordon, J., Michel, G., 2008. Analytical sensitivity limits for lateral flow immunoassays. Clinical chemistry 54, 1250–1251. https://doi.org/10.1373/clinchem.2007.102491.

Hampl, J., Hall, M., Mufti, N.A., Yao, Y.M., MacQueen, D.B., et al., 2001. Upconverting phosphor reporters in immunochromatographic assays. Analytical Biochemistry 288, 176–187. https://doi.org/10.1006/abio.2000.4902.

Heidenreich, A., Aus, G., Bolla, M., Joniau, S., Matveev, V.B., et al., 2008. EAU guidelines on prostate cancer. Eur. Urol. 53, 68–80 (doi:S0302-2838(07)01145-1 [pii]).

Jung, K., Zachow, J., Lein, M., Brux, B., Sinha, P., et al., 1999. Rapid detection of elevated prostate-specific antigen levels in blood: performance of various membrane strip tests compared. Urology 53, 155–160 (doi:S0090-4295(98)00419-1 [pii]).

Juntunen, E., Myyrylainen, T., Salminen, T., Soukka, T., Pettersson, K., 2012. Performance of fluorescent europium(III) nanoparticles and colloidal gold reporters in lateral flow bioaffinity assay. Anal. Biochem. 428, 31–38. https://doi.org/10.1016/j.ab.2012.06.005.

Juntunen, E., Arppe, R., Kalliomaki, L., Salminen, T., Talha, S.M., et al., 2015. Effects of blood sample anticoagulants on lateral flow assays using luminescent photon-up-converting and Eu(III) nanoparticle reporters. Anal. Biochem. 492, 13–20 (doi:S0003-2697(15)00439-X [pii]).

Koets, M., Sander, I., Bogdanovic, J., Doekes, G., van Amerongen, A., 2006. A rapid lateral flow immunoassay for the detection of fungal alpha-amylase at the workplace. Journal of environmental monitoring : JEM 8, 942–946. https://doi.org/10.1039/b605389k.

Lee, C.K., Cho, C.H., Woo, M.K., Nyeck, A.E., Lim, C.S., et al., 2012. Evaluation of Sofia fluorescent immunoassay analyzer for influenza A/B virus. Journal of clinical virology 55, 239–243. https://doi.org/10.1016/j.jcv.2012.07.008.

Leonardi, G.P., Wilson, A.M., Zuretti, A.R., 2013. Comparison of conventional lateral-flow assays and a new fluorescent immunoassay to detect influenza viruses. Journal of virological methods 189, 379–382. https://doi.org/10.1016/j.jviromet.2013.02.008.

Li, X., Li, W., Yang, Q., Gong, X., Guo, W., et al., 2014. Rapid and Quantitative Detection of Prostate specific Antigen with a Quantum Dot Nanobeads-based Immunochromatography Test Strip. ACS Appl. Mater. Interfaces 6, 6406–6414. https://doi.org/10.1021/am5012782.

Liang, R.L., Deng, Q.T., Chen, Z.H., Xu, X.P., Zhou, J.W., et al., 2017. Europium (III) chelate microparticle-based lateral flow immunoassay strips for rapid and quantitative detection of antibody to hepatitis B core antigen. Sci. Rep. 7, 14093. https://doi.org/10.1038/s41598-017-14427-4.

Lilja, H., Christensson, A., Dahlen, U., Matikainen, M.T., Nilsson, O., et al., 1991. Prostate-specific antigen in serum occurs predominantly in complex with alpha 1-antichymotrypsin. Clin. Chem. 37, 1618–1625.

Linares, E.M., Kubota, L.T., Michaelis, J., Thalhammer, S., 2012. Enhancement of the detection limit for lateral flow immunoassays: evaluation and comparison of bioconjugates. Journal of immunological methods 375, 264–270. https://doi.org/10.1016/j.jim.2011.11.003.

Liu, A., Zhao, F., Zhao, Y., Shangguan, L., Liu, S., 2016. A portable chemiluminescence imaging immunoassay for simultaneous detection of different isoforms of prostate specific antigen in serum. Biosens. Bioelectron. 81, 97–102. https://doi.org/10.1016/j.bios.2016.02.049.

Matsumoto, K., Konishi, N., Hiasa, Y., Kimura, E., Takahashi, Y., et al., 1999. A highly sensitive enzyme-linked immunoassay for serum free prostate specific antigen (f-PSA). Clin. Chim. Acta 281, 57–69. https://doi.org/10.1016/S0009-8981(98)00208-3.

Miano, R., Mele, G.O., Germani, S., Bove, P., Sansalone, S., et al., 2005. Evaluation of a new, rapid, qualitative, one-step PSA Test for prostate cancer screening: the PSA RapidScreen test. Prostate Cancer Prostatic Dis. 8, 219–223 (doi:4500802 [pii]).

Nabatiyan, A., Baumann, M.A., Parpia, Z., Kelso, D., 2010. A lateral flow-based ultrasensitive p24 HIV assay utilizing fluorescent microparticles. Journal of acquired immune deficiency syndromes(1) 53, 55–61. https://doi.org/10.1097/QAI.0b013e3181c4b9d5.

Parpia, Z.A., Elghanian, R., Nabatiyan, A., Hardie, D.R., Kelso, D.M., 2010. p24 antigen rapid test for diagnosis of acute pediatric HIV infection. Journal of acquired immune deficiency syndromes 55, 413–419. https://doi.org/10.1097/QAI.0b013e3181f1afbc.

Peltola, M.T., Niemela, P., Alanen, K., Nurmi, M., Lilja, H., et al., 2011. Immunoassay for the discrimination of free prostate-specific antigen (fPSA) forms with internal cleavages at Lys((1)(4)(5)) or Lys((1)(4)(6)) from fPSA without internal cleavages at Lys((1)(4)(5)) or Lys((1)(4)(6)). Journal of immunological methods 369, 74–80. https://doi.org/10.1016/j.jim.2011.04.006.

Pettersson, K., Piironen, T., Seppala, M., Liukkonen, L., Christensson, A., et al., 1995. Free and complexed prostate-specific antigen (PSA): in vitro stability, epitope map, and development of immunofluorometric assays for specific and sensitive detection of free PSA and PSA-alpha 1-antichymotrypsin complex. Clin. Chem. 41, 1480–1488.

Preechakasedkit, P., Osada, K., Katayama, Y., Ruecha, N., Suzuki, K., et al., 2018. Gold nanoparticle core-europium(iii) chelate fluorophore-doped silica shell hybrid nanocomposites for the lateral flow immunoassay of human thyroid stimulating hormone with a dual signal readout. Analyst 143, 564–570. https://doi.org/10.1039/c7an01799e.

Rajakoski, K., Piironen, T., Pettersson, K., Lovgren, J., Karp, M., 1997. Epitope mapping of human prostate specific antigen and glandular kallikrein expressed in insect cells. Prostate cancer and prostatic diseases 1 16–20. https://doi.org/10.1038/sj.pcan.4500206.

Rundstrom, G., Jonsson, A., Martensson, O., Mendel-Hartvig, I., Venge, P., 2007. Lateral flow immunoassay using Europium (III) chelate microparticles and time-resolved fluorescence for eosinophils and neutrophils in whole blood. Clin. Chem. 53, 342–348 (doi:clinchem.2006.074021 [pii]).

Salminen, T., Knuutila, A., Barkoff, A.M., Mertsola, J., He, Q., 2018. A rapid lateral flow immunoassay for serological diagnosis of pertussis. Vaccine 36, 1429–1434. https://doi.org/10.1016/j.vaccine.2018.01.064.

Scherr, T., Gupta, S., Wright, D., Haselton, F., 2016. Mobile phone imaging and cloud-based analysis for standardized malaria detection and reporting. Scientific Reports 27.

Shao XY, Wang CR, Xie CM, Wang XG, Liang RL, et al. (2017) Rapid and Sensitive Lateral Flow Immunoassay Method for Procalcitonin (PCT) based on Time-Resolved Immunochromatography. Sensors (Basel) 17. doi:https://doi.org/10.3390/s17030480.

Sharma, S., Zapatero-Rodríguez, J., O'Kennedy, R., 2017. Prostate cancer diagnostics: Clinical challenges and the ongoing need for disruptive and effective diagnostic tools. Biotechnol. Adv. 35, 135–149. https://doi.org/10.1016/j.biotechadv.2016.11.009.

Song, X., Knotts, M., 2008. Time-resolved luminescent lateral flow assay technology. Anal. Chim. Acta 626, 186–192. https://doi.org/10.1016/j.aca.2008.08.006.

Song, C., Zhi, A., Liu, Q., Yang, J., Jia, G., et al., 2013. Rapid and sensitive detection of β-agonists using a portable fluorescence biosensor based on fluorescent nanosilica and a lateral flow test strip. Biosens. Bioelectron. 50, 62–65. https://doi.org/10.1016/j.bios.2013.06.022.

Soukka, T., Harma, H., Paukkunen, J., Lovgren, T., 2001a. Utilization of kinetically enhanced monovalent binding affinity by immunoassays based on multivalent nanoparticle-antibody bioconjugates. Anal. Chem. 73, 2254–2260.

Soukka, T., Paukkunen, J., Harma, H., Lonnberg, S., Lindroos, H., et al., 2001b. Supersensitive time-resolved immunofluorometric assay of free prostate-specific antigen with nanoparticle label technology. Clin. Chem. 47, 1269–1278.

Stephan, C., Ralla, B., Jung, K., 2014. Prostate-specific antigen and other serum and urine markers in prostate cancer. Biochimica et Biophysica Acta (BBA) - Reviews on Cancer 1846, 99–112. https://doi.org/10.1016/j.bbcan.2014.04.001.

Tilki, D., Kim, S.I., Hu, B., Dall'Era, M.A., Evans, C.P., 2015. Ultrasensitive Prostate specific Antigen and its Role after Radical Prostatectomy: a Systematic Review. J. Urol. 193, 1525–1531. https://doi.org/10.1016/j.juro.2014.10.087.

van Dam, G.J., Wichers, J.H., Ferreira, T.M., Ghati, D., van Amerongen, A., et al., 2004.

Diagnosis of schistosomiasis by reagent strip test for detection of circulating cathodic antigen. Journal of clinical microbiology 42, 5458–5461 (42/12/5458 pii).

Xia, X., Xu, Y., Zhao, X., Li, Q., 2009. Lateral Flow Immunoassay using Europium Chelate-Loaded Silica Nanoparticles as Labels. Clin. Chem. 55, 179–182. https://doi.org/10.1373/clinchem.2008.114561.

Xia, X., Xu, Y., Ke, R., Zhang, H., Zou, M., et al., 2013. A highly sensitive europium nanoparticle-based lateral flow immunoassay for detection of chloramphenicol residue. Anal. Bioanal. Chem. 405, 7541–7544. https://doi.org/10.1007/s00216-013-7210-9.

Xu, H., Chen, J., Birrenkott, J., Zhao, J.X., Takalkar, S., et al., 2014. Gold-Nanoparticle-decorated Silica Nanorods for Sensitive Visual Detection of Proteins. Anal. Chem. 86, 7351–7359. https://doi.org/10.1021/ac502249f.

Yousef, G.M., Diamandis, E.P., 2002. Expanded human tissue kallikrein family–a novel panel of cancer biomarkers. Tumour Biol. 23, 185–192. https://doi.org/10.1159/000064027.

Zhang, F., Zou, M., Chen, Y., Li, J., Wang, Y., et al., 2014. Lanthanide-labeled immunochromatographic strips for the rapid detection of Pantoea stewartii subsp. stewartii. Biosensors & bioelectronics 51, 29–35. https://doi.org/10.1016/j.bios.2013.06.065.